Capillary Flow of Discotic Nematic Liquid Crystals' Onion Textures

Luiz R.P. de Andrade Lima; Alejandro D. Rey
Department of Chemical Engineering, McGill University
3610 University Street, Montreal, Quebec, Canada H3A 2B2
e-mail: ldeand@po-box.mcgill.ca; alejandro.rey@mcgill.ca

Abstract

Highly filled clay-based polymer nano-composites are expected to display discotic nematic ordering. In this study, the Poiseuille capillary flow of discotic nematic liquid crystals is analyzed using the Ericksen-Leslie theory, for three families of static patterns known as escaped and defect core onion textures, defined by the orientation at the capillary' centerline. The escaped textures have low-elastic energy and high dissipation cores. The defect core texture has a high elastic energy-low dissipation core. The Poiseuille flow of these textures exhibits non-parabolic velocity profiles and their apparent viscosities display shear thickening, with exponents close to $1/5 \pm 0.07$. It is found that core conditions have a strong effect on the Non-Newtonian rheology of discotic nematics displaying the onion texture. We expect that the present work will be of practical utility to the currently intense investigation of the rheology and processing flows of polymer nano-composites.

Introduction

Liquid crystals are anisotropic viscoelastic materials, whose essential characteristic is orientation elasticity. Elastic storage arises in the presence of spatial orientation gradients, whose magnitude becomes considerable at small length scales, such as in thin fibers in the micron range where the propagation of the surface curvature into the inner layers creates strong orientation gradients. In this case high elastic energy can be avoided by two director orientation mechanisms: director escape from the 2D planar orientation layer into a 3D orientation, and defect nucleation in a planar 2D orientation layer. The orientation escape mechanism may sometimes be frustrated by fixed boundary conditions and/or flow effects, and defect structures may then result. Escape mechanisms lead to 3D orientation structures of finite macroscopic size while the defect cores of planar orientation fields have molecular sizes. The flow behavior and rheological material functions of escaped 3D textures and defect textures are of fundamental significance to control and optimize the nematic liquid crystal texture formation [1,2].

This paper presents an analysis for the capillary Poiseuille flow of the frequently observed onion texture of DNLCs (see Fig. 1). The director field in the onion texture is mainly radial, the average molecular orientation being azimuthal, and splay is the main elastic deformation. In this planar orientation the splay energy diverges at the centerline and the structure either nucleates a defect of molecular size r_c or escapes the cross-sectional plane towards the axial direction [3,4]. Since the director escape can be into the positive or negative axial direction, two escaped 3D orientation structures of finite size are possible, henceforth denoted as E+ and E-, where in the E+ the director at the centerline is **n**=(0,0,+1), and for E- it is **n**=(0,0,-1). The onion texture with a defect at the centerline is denoted by D_c. The defect in the D_c texture is an edge disclination line of strength S=+1 [3]. The term edge means that the defect is perpendicular to the director field; the term disclination is used to denote orientational

defects, and the strength S quantifies the amount of rotation of the director when following a path encircling the defect, and the sign of S denotes the sense of rotation. Since the orientation fields of the core regions in the E+, E-, and D_c textures are different the imposition of a flow field will lead to further distinctions in the flow behavior and in their viscosity functions.

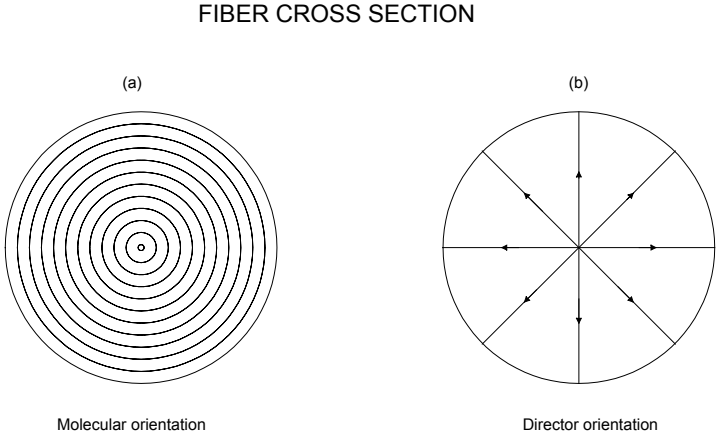

Figure 1. Schematic representation of the disc trajectories (a) and director orientation (b) in the onion textures' cross section.

This paper, uses the anisotropic viscoelastic Ericksen-Leslie theory adapted to DNLCs, characterizes the velocity and the orientation behavior of discotic nematic liquid crystals in Poiseuille flow displaying the escaped (E-, E+) onion textures, and the defect (D_c) onion texture, and presents the effect of the different onion textures on the non-Newtonian flow behavior.

Governing Equations

In flowing liquid crystal systems, elastic and viscous stresses are usually both important. The continuum theory of elasticity of liquid crystals takes into account external forces that distort the spatially uniform equilibrium configurations of liquid crystals. For Poiseuille capillary flow, using cylindrical coordinate system, Fig.2, axisymmetric planar director field ($\mathbf{n}(r,t)=(\sin\theta(r,t),0,\cos\theta(r,t))$) and purely axial velocity field ($\mathbf{v}(r,t)=(0,0,v(r,t))$) the steady dimensionless governing equations for the director tilt angle $\theta(\tilde{r},\tilde{t})$ and the axial velocity $\tilde{v}(\tilde{r},\tilde{t})$ are [5,6,7]:

$$\left(\cos^2\theta+\varepsilon\sin^2\theta\right)\left(\frac{d^2\theta}{d\tilde{r}^2}+\frac{1}{\tilde{r}}\frac{d\theta}{d\tilde{r}}\right)+\frac{\sin 2\theta}{2}\left[(\varepsilon-1)\left(\frac{d\theta}{d\tilde{r}}\right)^2-\frac{1}{\tilde{r}^2}\right]+\left[\frac{\tilde{\gamma}_1}{4\tilde{\eta}(\theta)}\left(1-\frac{\cos 2\theta}{\cos 2\theta_s}\right)\mathrm{Er}\right]\tilde{r}=0 \qquad (1)$$

$$\frac{d\tilde{v}}{d\tilde{r}}+\frac{\mathrm{Er}}{2\tilde{\eta}(\theta)}\tilde{r}=0 \qquad (2)$$

$$\tilde{\eta}(\theta)=(\tilde{\alpha}_1/4)\sin^2 2\theta+\tilde{\eta}_2\sin^2\theta+\tilde{\eta}_1\cos^2\theta\ , \qquad (3)$$

$$\tilde{\eta}_1=\eta_1/\overline{\eta}\ , \qquad \tilde{\eta}_2=\eta_2/\overline{\eta}\ , \qquad \tilde{\gamma}_1=\gamma_1/\overline{\eta}\ , \qquad \tilde{\alpha}_i=\alpha_i/\overline{\eta} \qquad (4a,b,c,d)$$

where a tilda signifies a dimensionless variable, $\varepsilon = K_{33}/K_{11}$ is the ratio of the bend and the splay Frank elastic constants, $\tilde{v} = \bar{\eta} R\, v/K_{11}$ is the dimensionless velocity, $Er = R^3(-dp/dz)/K_{11}$ is the ratio of viscous flow effects to long-range elasticity effects known as the Ericksen number, $\tilde{r} = r/R$ is the dimensionless radial distance, dp/dz is the given pressure drop in the capillary per unit length, $\tilde{\alpha}_i$ are the dimensionless Leslie viscosities, θ_s is the stable flow-alignment Leslie angle,

$$\theta_s^m = m\pi + 1/2\cos^{-1}(1/\lambda), \qquad m = 0,1,2,... \tag{5}$$

The expression for θ_s corresponds to negative shear rates relevant to this paper; For DNLCs the reactive parameter (λ) is negative, and the director orientation aligns in the shear plane close to the velocity gradients if $\lambda<-1$. Note that in deriving Eqs. (1) and (2), the velocity gradient at the centerline is assumed to be finite. Since r_c is a molecular length scale, the equations are also applicable for the D_c texture.

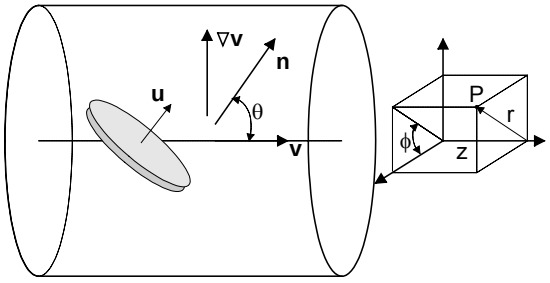

Figure 2. Schematic representations of the flow in a capillary showing an uniaxial disc-like molecules with unit normal vector (**u**), director vector (**n**), velocity vector (**v**), velocity gradient (∇**v**), alignment angle (θ) and the cylindrical (r,ϕ,z) coordinate system used to describe a generic point P.

The director orientation (Eq. (1)) is a non-linear 2nd order ordinary differential equation, whereas the equation for the axial velocity is first order. The director orientation boundary conditions used for the three textures are

$$E+:\ \theta(0) = 0,\ \theta(1) = \pi/2;\ \ E-:\ \theta(0) = \pi,\ \theta(1) = \pi/2\ ;\ \ D_c:\ \theta(\tilde{r}_c) = \pi/2,\ \theta(1) = \pi/2 \tag{6}$$

At the centerline the director orientation for the escaped textures is along the fiber axis, and for the defect core texture it is radial. At the pipe wall the director orientation for all three textures is homeotropic ($\theta(1)=\pi/2$). In previous work for Poiseuille flow of rod-like nematic liquid crystals [5] the boundary condition at the centerline was that of the E+ texture. The solutions to the governing Eqs. (1) and (2) subjected to boundary conditions given by Eq. (6) have finite elastic energy. For the $E\pm$ textures the director escapes the shear plane to decrease the splay elastic energy [3]. For the D_c defect texture the elastic energy remains finite because $r_c>0$. For the D_c texture the boundary condition is applied at the edge of the defect core, which is of molecular dimensions. Using typical sizes one assumes $\tilde{r}_c = 5 \times 10^{-4}$. For the axial velocity we use the no slip condition at the bounding surface: $\tilde{v}(1) = 0$

The dimensionless flow-rate $\widetilde{Q}$ in Poiseuille capillary flow, that is useful in discussing the non-Newtonian rheology, is calculated by the integration of the dimensionless axial velocity profile. Using the classical definition of apparent viscosity for Poiseuille capillary flow the following dimensionless apparent viscosity appropriate for a DNLC is obtained:

$$\widetilde{\eta}_{app} = \frac{\pi \, Er}{8 \widetilde{Q}} \tag{7}$$

Equation (1) is solved numerically using the Galerkin Finite Element method. The integrals were computed using three points Gaussian quadrature and the resulting set of non-linear equations are solved using the Newton-Raphson iteration scheme. Convergence is assumed to occur when the length of the difference between two successive solutions vectors is less than 10^{-10}. The velocity profile and the flow-rate in the capillary are calculated by using Gaussian quadrature integration. Mesh independence was established using standard mesh refinement criteria [8]. The computations are performed for a set of characteristic DNLCs parameters listed in Table 1, which correspond to the six scaled Leslie coefficients calculated from non-equilibrium molecular dynamics simulations and the Frank elastic constants measured to hexakis(dodecanoyloxy)truxene [9]. The essential features of the solutions and the main conclusions of this paper will remain unaffected if one uses other parametric values corresponding to flow-aligning DNLCs.

Numerical results and discussion

This section presents the computed director orientation and dimensionless axial velocity profiles as a function of the Ericksen number for the three onion textures studied here. As $Er \to \infty$ the two stable $\left(\theta_s^1, \theta_s^3\right)$ and the unstable $\left(\theta_u^2, \theta_u^4\right)$ Leslie angles that satisfy Eqs. (1) and (2) are given by:

$$\theta_s^1 = 1/2 \cos^{-1}\left(1/\lambda\right) \;\; ; \;\; \theta_s^3 = \pi + 1/2 \cos^{-1}\left(1/\lambda\right) \;\; ; \;\; \theta_u^2 = \pi - 1/2 \cos^{-1}\left(1/\lambda\right) \;\; ; \;\; \theta_u^4 = 2\pi - 1/2 \cos^{-1}\left(1/\lambda\right) \tag{8a,b,c,d}$$

The superscripts in the Leslie angles (1-4) correspond to the quadrant in the unit circle. In the present case the shear rate is negative ($dv/dr<0$), thus the flow alignment angle lies in the 1st (or equivalently 3^{d}) quadrant. For the E+ and D_c onion textures the flow tend to align **n** in the first quadrant ($\theta \to \theta_s^1 = 1.157$), while for the E- the two stable Leslie angles are possible. Nevertheless since in pipe flow the viscous torques are zero (maximum) at the centerline (wall) the bias is towards the stable Leslie angle θ_s^1 in the first quadrant ($\theta \to \theta_s^1 = 1.157$). The axial orientation is associated with the highest viscosity and the lowest elasticity. The radial direction is associated with the highest elasticity and lowest viscosity. The flow torques promote orientation close to the radial direction. Poiseuille flow is a non-homogeneous shear flow, with zero shear rate at the centerline, thus for a given Ericksen number the flow effect on orientation is a maximum at the pipe wall and minimum at the centerline.

The computed director orientation θ as a function of dimensionless radial distance $\tilde{r}$, for the three onion textures, for increasing elastic anisotropy ratio ε, under static conditions (Er=0) indicated that director behavior for the escaped and defect core textures in the absence of flow: the director field of the D_c texture is independent ε, as ε increases the director of the E textures gets closer and closer to the D_c texture, as ε increases the director profile of the E

textures displays large gradients close to the centerline, and the director profiles for the E textures are symmetric with respect to $\pi/2$.

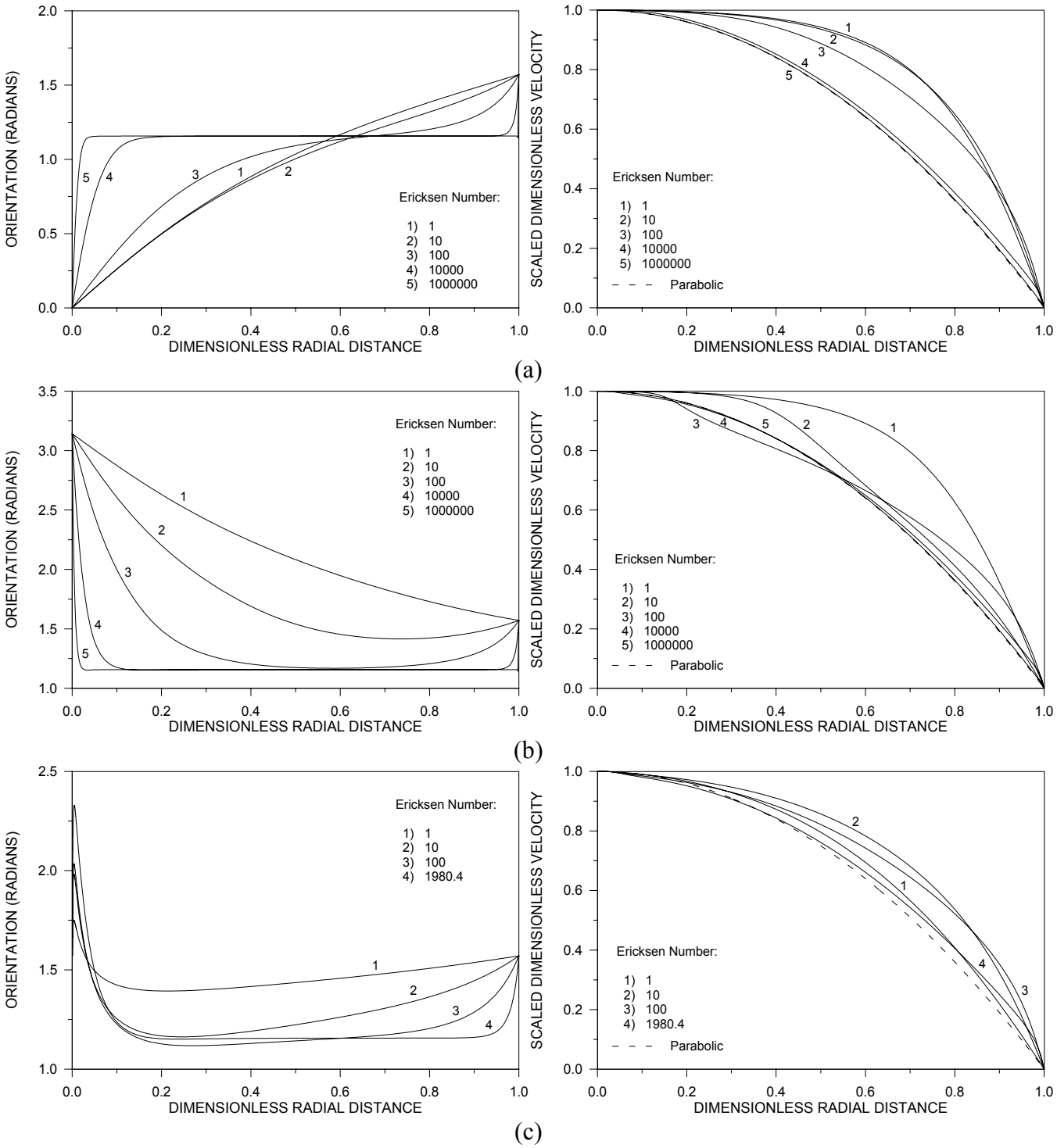

Figure 3: Director orientation and velocity as a function of the dimensionless radial distance ($\tilde{r}$) for: (a) escaped (E+), (b) escaped (E-), and (c) defect (D_c) onion textures, for increasing Ericksen number (Er).

Fig. 3 shows the orientation θ and the corresponding dimensionless axial velocity profiles, for increasing Er for the E+, E-, and D_c onion textures. The top figure shows that as Ericksen number increases above a thousand, boundary layer behavior is observed, with most of the cross-section aligned along the stable Leslie angle $\theta_s^1 = 1.157$. There are two boundary layers, one in the centerline region of thickness δ_c and another of thickness δ_w at the pipe wall region. As Er increases δ_c decreases at a slower rate than δ_w because the flow effect is stronger at the pipe wall and because the elastic effect promotes the axial orientation at the centerline. The middle figure shows that in the E- texture the flow effect cooperates with elasticity in the sector (θ_u^2, π) increasing δ_c in comparison with the E+ textures. The bottom figure shows the flow effect on the D_c onion texture. As Er increases an escaped core region, where the director escapes towards the low energy axial $(\theta=\pi)$ orientation, appears. As the director escapes the shear plane, the elastic energy at the centerline region decreases. The deviation of the director from the radial orientation measures the amplitude of the escape process. Fig. 3c shows that as Er increases the amplitude increases. At sufficiently high Er, the director angle is greater than θ_u^2 and flow tends to align the director along θ_s^1 in the bulk region, creating sharp gradients. As Er increases the director gradient incurs large increases, thus requiring finer and finer meshes for convergence. We have obtained converged mesh-independent solutions up to Er=1980. The sharp gradients-high elastic energy state indicate that the system may likely be unstable to director orientation changes, defect core size changes, and/or defect core structure changes. Defect core size and structure processes are not captured by this model. For the dimensionless axial velocity profiles on remarks that the profiles deviate from the parabolic Newtonian profile because the local viscosity $\tilde{\eta}(\theta)$ (defined in Eq. (3)) is spatially non-homogeneous, and the higher the overall variation of $\tilde{\eta}(\theta)$ the higher the deviation from the Newtonian parabolic velocity behavior ($\tilde{v} = 1 - \tilde{r}^2$).

A hall mark of liquid crystal rheology is the interaction between orientation and velocity, which underlie their characteristic Non-Newtonian behavior. In this section we characterize the Non-Newtonian rheology using Eq. (7). In the present shear Poiseuille flow (α_1=0) the local scaled orientation viscosity $\tilde{\eta}\left(\theta\left(\tilde{r}\right)\right)$ obtained from the Ericksen-Leslie theory (Eq. (3)) is given by:

$$\tilde{\eta}\left(\theta\left(\tilde{r}\right)\right) = \tilde{\eta}_l + \left(\tilde{\eta}_2 - \tilde{\eta}_l\right)\sin^2\theta\left(\tilde{r}\right) \tag{8}$$

According to Eq. (7), the dimensionless apparent viscosity $\tilde{\eta}_{app}$ is a function of the local scaled orientation viscosity $\tilde{\eta}\left(\theta(\tilde{r})\right)$ the Non-Newtonian rheology is driven by the averaged $\tilde{\eta}\left(\theta(\tilde{r})\right)$.

For sufficiently small and very large Er numbers we expect and find, Newtonian viscosity plateaus. As $\mathrm{Er} \to \infty$ for λ<-1 all the directors align along the stable Leslie angle and the apparent viscosity is then the alignment viscosity:

$$\lim_{\mathrm{Er}\to\infty} \tilde{\eta}_{app}(\mathrm{Er}) = \tilde{\eta}(\theta_s) = \tilde{\eta}_l + (\tilde{\eta}_2 - \tilde{\eta}_l)\sin^2\theta_s^1 \quad ; \quad \theta_s^1 = 1/2\cos^{-1}(1/\lambda) \tag{9}$$

For the present case $\lim_{\mathrm{Er}\to\infty}\tilde{\eta}_{\mathrm{app}}(\mathrm{Er})=0.465$. For infinitesimal Er the original textures are unperturbed. For the D_c texture the zero shear rate Newtonian plateau is

$$\lim_{\mathrm{Er}\to 0}\tilde{\eta}_{\mathrm{app}\,D_c}(\mathrm{Er})=\tilde{\eta}(\theta=\pi/2)=\tilde{\eta}_2 \tag{10}$$

For the present case $\lim_{\mathrm{Er}\to 0}\tilde{\eta}_{\mathrm{app}D_c}(\mathrm{Er})=0.124$. For the E textures the computation of the zero shear rate Newtonian plateau is more complicated because θ varies with r but an analytical expression is obtained for ε=1, that gives:

$$\lim_{\mathrm{Er}\to 0}\tilde{\eta}_{\mathrm{app}\,E_+}(Er)=\lim_{\mathrm{Er}\to 0}\tilde{\eta}_{\mathrm{app}\,E_-}(Er)=\tilde{\eta}\left(\theta=2\tan^{-1}(\tilde{r})\right)= \tag{11}$$

$$=\tilde{\eta}_1\left\{1+8\left(1-\frac{\tilde{\eta}_2}{\tilde{\eta}_1}\right)\left[1+\left(1-2\frac{\tilde{\eta}_2}{\tilde{\eta}_1}\right)\ln\left(4\frac{\tilde{\eta}_2}{\tilde{\eta}_1}\right)+2\frac{\frac{\tilde{\eta}_1}{\tilde{\eta}_2}\left(\frac{1}{2}-\frac{\tilde{\eta}_2}{\tilde{\eta}_1}\right)^2-\left(1-\frac{\tilde{\eta}_2}{\tilde{\eta}_1}\right)}{\sqrt{\frac{\tilde{\eta}_1}{\tilde{\eta}_2}-1}}\tan^{-1}\left(\sqrt{\frac{\tilde{\eta}_1}{\tilde{\eta}_2}-1}\right)\right]\right\}^{-1}$$

Since for DNLCs the inequality $\eta_1 > \eta_2$ holds, use of Eq. (11) leads to the following general result:

$$\lim_{\mathrm{Er}\to 0}\tilde{\eta}_{\mathrm{app}\,E_+}(\mathrm{Er})=\lim_{\mathrm{Er}\to 0}\tilde{\eta}_{\mathrm{app}\,E_-}(\mathrm{Er})>\tilde{\eta}_2 \tag{12}$$

This general result is obtained by setting $\tilde{\eta}_1=a\,\tilde{\eta}_2$ ($a\geq 1$) and evaluating Eq. (11). For ε=1.64 the numerical solutions gives $\lim_{\mathrm{Er}\to 0}\tilde{\eta}_{\mathrm{app}\,E_+}(Er)=\lim_{\mathrm{Er}\to 0}\tilde{\eta}_{\mathrm{app}\,E_-}(Er)=0.180$ and for ε=1 the analytical solution Eq. (11) gives $\lim_{\mathrm{Er}\to 0}\tilde{\eta}_{\mathrm{app}\,E_+}(\mathrm{Er})=\lim_{\mathrm{Er}\to 0}\tilde{\eta}_{\mathrm{app}\,E_-}(\mathrm{Er})=0.199$. Based on Eqs. (10) and (12) we find that when $\tilde{\eta}_1 > \tilde{\eta}_2$ the following onion texture viscosity ordering results:

$$\lim_{\mathrm{Er}\to 0}\tilde{\eta}_{\mathrm{app}\,D_c}(\mathrm{Er})<\lim_{\mathrm{Er}\to 0}\tilde{\eta}_{\mathrm{app}\,E_+}(\mathrm{Er})=\lim_{\mathrm{Er}\to 0}\tilde{\eta}_{\mathrm{app}\,E_-}(\mathrm{Er})<\lim_{\mathrm{Er}\to\infty}\tilde{\eta}_{\mathrm{app}}(\mathrm{Er}) \tag{13}$$

For the present case the inequalites are: $0.124<0.180<0.465$. Thus for all DNLCs onion textures considered here the rheology is characterized by viscosity shear thickening behavior.

Fig. 4 shows the computed dimensionless apparent viscosity $\tilde{\eta}_{\mathrm{app}}$ as a function of the Ericksen number for the three onion textures, and ε=1.64. The simulations are in agreement with the theoretical ordering Eq. (13). The apparent viscosity of all textures display shear thickening, with exponents close to $1/5\pm 0.07$. The shear thickening behavior arises from the characteristic ordering of the shear Miesowicz viscosities of discotic nematic liquid crystals. The viscosity function of the onion texture with an escaped orientation core that funnels away from the flow direction shows a low shear rate Newtonian plateau, followed by a shear thinning region, a shear thickening region, and a high shear rate Newtonian plateau. The shear thinning arises from the escaped orientation core. The viscosity function of the onion texture with an escaped orientation core that funnels towards the flow direction shows a low shear rate

Newtonian plateau, followed by a shear thickening region, and a high shear rate Newtonian plateau. The viscosity function of the defect core onion texture shows a low shear rate Newtonian plateau, followed by a shear thickening region. The apparent viscosity becomes independent of the texture only at Er >1000.

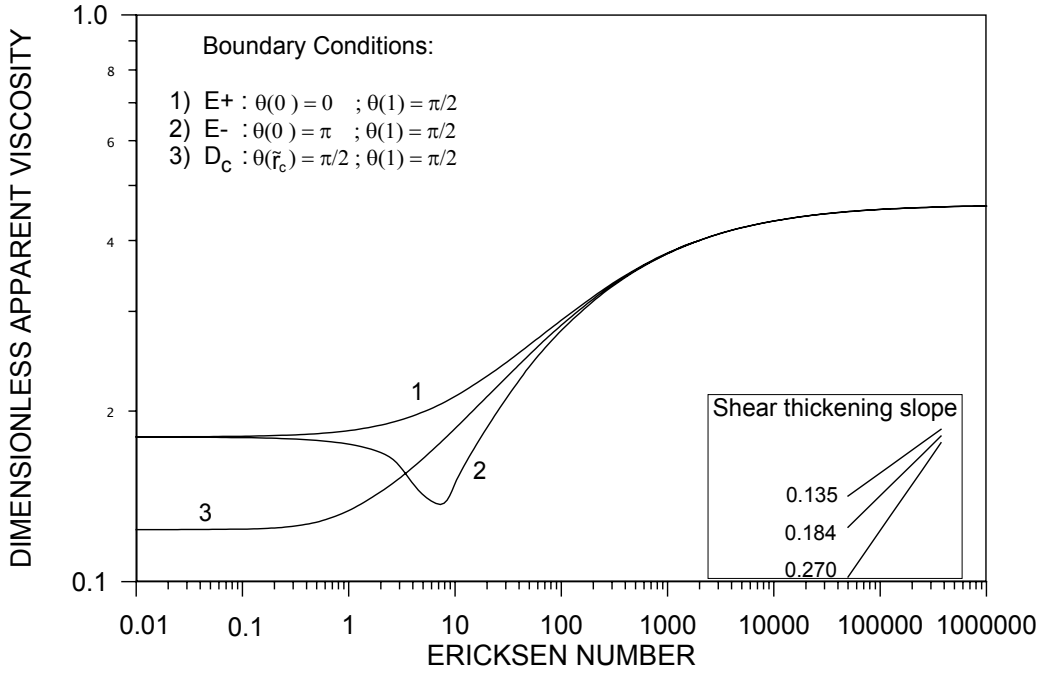

Figure 4. Dimensionless apparent viscosity ($\tilde{\eta}$) as a function of the Ericksen number (Er) for the escaped (1: E+ and 2: E-) and defect (3: D_c) onion textures.

Conclusions

The Poiseuille capillary flow of discotic nematic liquid crystals has been analyzed using the Ericksen-Leslie equations and material parameters corresponding to these particular liquid crystals. Three families of static patterns known as escaped and defect core onion textures are identified according to the orientation at the capillary' centerline. The escaped textures have low-elastic energy and high dissipation cores. The defect core texture has a high elastic energy-low dissipation core. The Poiseuille flow of these textures exhibits non-parabolic velocity profiles due to the underlying orientation gradients. The apparent viscosity of all the textures display shear thickening, with exponents close to 1/5. Up to an Ericksen number of a thousand, core conditions have a strong effect on the non-Newtonian rheology of discotic nematics displaying the onion texture.

Acknowledgments

This research was supported by a grant from Engineering Research Center program of National Science Foundation under award number EEC 9731680. One of us (LRPdAL) gratefully acknowledges the support of Natural Sciences and Engineering Research Council of Canada, and Eugenie Ulmer Lamothe Scholarship Fund (Department of Chemical Engineering, McGill University).

References

[1] Rey, A.D. and M.M. Denn, “Dynamical phenomena in liquid-crystalline materials”, Annual Reviews in Fluid Mechanics, **34**, 233 (2002).

[2] Chandrasekhar, S., Liquid Crystals, 2nd edn. Cambridge: Cambridge University Press. 1992.

[3] P.G. de Gennes, J. Prost, The Physics of Liquid Crystals, 2nd edn. London: Oxford University Press. 1993.

[4] P.E. Cladis and M. Kleman, Non-singular disclinations of strength S=+1 in nematics, J. de Physique 33 (1972) 591.

[5] H.C. Tseng, D.L. Silver, B.A Finlayson, Application of the continuum theory to nematic liquid crystals, Phys. Fluids 15:7 (1972) 1213.

[6] L.R.P.de Andrade Lima, A.D. Rey, “Poiseuille flow of Leslie-Ericksen discotic liquid crystals: solution mutliplicity, multistability, and non-newtonian rheology”, *Journal of Non-Newtonian Fluid Mechanics*, **110**(2-3), 103, 2003.

[7] L.R.P. de Andrade Lima and A.D. Rey, “Computational Modeling of Ring Textures in Mesophase Carbon Fibers”, *Materials Research*, 6(2), 285-293, 2003.

[8] C.A.J. Fletcher, *Computational Techniques for Fluid Dynamics 1: Fundamental and General Techniques,* (Springer-Verlag: New York, 1996).

[9] A.S.K. Ho, A.D. Rey, Orienting properties of discotic nematic liquid crystals in Jeffrey-Hamel flows, Rheol. Acta. 30 (1991) 77.